

Local high-temperature plasma formations in a high-current pinching discharge

Yu. A. Bykovskii and V. B. Lagoda

Moscow Engineering-Physics Institute

(Submitted 15 January 1980)

Zh. Eksp. Teor. Phys. **83**, 114–125 (July 1982)

Local high-temperature plasma formations produced in a high-current vacuum discharge with an initial stored energy of kJ and initiated by a plasma created by the focused radiation from a pulsed laser are investigated. The collapsing current-carrying plasma is found to split into separate current filaments. A mechanism of current-energy transfer to the plasma in the region where the filaments are linked is proposed on the basis of a model of self-stabilized plasma vortices produced when the current-carrying plasma moves in an external magnetic field. As a confirmation of the mechanism, some results are presented of an investigation of the microwave radiation and accelerated particles from the local high-temperature plasma formation region.

PACS numbers: 52.50. — b, 52.40.Kh, 52.80.Up, 52.25.Ps

INTRODUCTION

Local high-temperature plasma formations (LHPF) that have, besides a sharply outlined boundary of the hot region, extremely high electron densities ($n_e \sim 10^{20} - 10^{22} \text{ cm}^{-3}$) and electron temperature ($T_e \sim 1 - 10 \text{ keV}$) are observed in a number of devices in which a high-temperature plasma is obtained via pinching the current channel by the azimuthal magnetic self-field.¹⁻³ A typical approach to an explanation of the onset of LHPF is to analyze the evolution of a neck ($m = 0$) in a locally homogeneous pinching current-carrying plasma column.⁴ Next, to explain the experimentally observed phenomena (high-energy input to the plasma, intense fluxes of microwave and of soft and hard x-rays, high-energy ion and electron beams, anomalous plasma resistance) one resorts to such mechanisms as heating of the particles of the electrode material in the current channel,⁵ focusing of the high-energy electron beam in the plasma,⁶ radiative collapse followed by Fermi condensation of the electrons to the degenerate state,⁷ and others.

In the present paper we show, on the basis of an experimental study of a high-current laser-initiated vacuum discharge, that the onset of LHPF is the consequence of the existence of the fine structure in the collapsing current-carrying plasma. We investigate the parameters of the LHPF in the interelectrode-gap region that is most favorable for their onset. A model of the energy transfer to the plasma is proposed, based on consideration of the process of joining of several current filaments that make up the fine structure. The results of an investigation of microwave radiation and of the accelerated particles from the LHPF region are cited as confirmation of the proposed model.

EXPERIMENTAL SETUP

The discharge circuit consisted of a low-inductance 24- μF capacitor connected directly to coaxial electrodes placed in a vacuum chamber. The diameters of the inner (E_1) and outer (E_2) electrodes [Fig. 1(a)] were 15 and 30 mm, respectively. The distance from the end face of E_1 to the plane of the end face of E_2 was 8 mm.

An annular acute-angle ledge on E_1 , at the point of intersection of the cylindrical and conical generators, produced a region of increased electric field intensity, in which a current sheath was produced. A recess on the end face of E_1 ensured sagging of the current sheath at the instant of collapse, in analogy with the stage of transition to the inner surface of the central electrode in case of a Mather-geometry plasma focus with hollow anode.⁸ Observation of the region of the interelectrode gap was through an opening in the coaxial part of E_2 . The maximum discharge current (I_{max}) was 200 kA at an initial capacitor voltage 14 kV. Any electrode polarity could be investigated. The duration of the quarter-cycle of the discharge was 2 μsec . The energy of the initi-

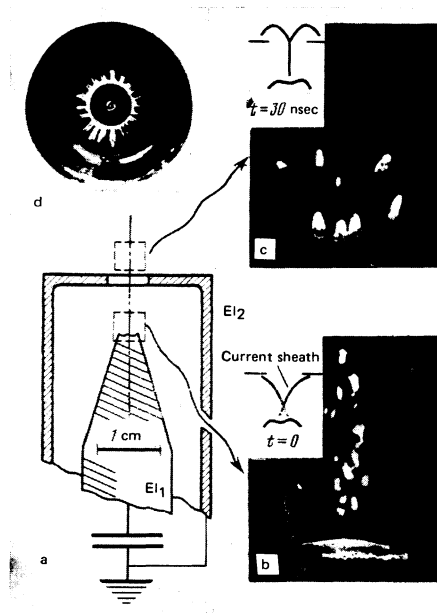


FIG. 1. a) Arrangement of electrodes; b, c) pin-point photographs of the electrode regions (exposure integrated over 30 discharges, cut-off energy of the pinpoint camera filters 2 keV, hole diameter 50 μm); d) photograph of the outer end face of the E_2 after three discharges, tracks of the current filaments on the sputtered lead film can be seen.

ing-laser pulse (wavelength $1.06 \mu\text{m}$) was 5 J at a duration 30 nsec. The laser radiation was focused through a central opening in El_2 onto the end face of El_1 by a lens of 120-mm focal length. The angle between the axis of the initiating radiation and the electrode axis was 14° . Electrodes El_1 and El_2 were made of the same material, namely pure metals with atomic numbers from 13 to 82, and installed simultaneously in the chamber. A vacuum $\sim 10^{-6}$ Torr was maintained in the interelectrode gap.

INVESTIGATION OF THE DYNAMICS AND STRUCTURE OF A CURRENT-CARRYING PLASMA

The investigated phenomenon, the formation of a high-temperature dense plasma, was observed near the axis during the first quarter-cycle of the discharge, in the course of a transition from a state at which the discharge current is distributed over a considerable fraction of the plasma-filled interelectrode gap to a state of contracted self-maintaining arc discharge. The discharge current and its derivative with respect to time were measured with calibrated Rogowski loops. The visible glow of the plasma recorded with an electron-optical camera yielded the current density in the interelectrode volume. The frame exposure time was 40 nsec and made possible a spatial resolution of $\sim 700 \mu\text{m}$. To investigate the fine structure of the current sheath with large spatial resolution, we used the evaporating-coatings procedure.⁹ The internal and external end surfaces of El_2 were laser-coated by a metal film several microns thick. In the course of the discharge, this film was locally evaporated at the points with increased current density. The image obtained in this manner was an analog of photographs produced when high-speed processes are recorded with a streak camera,¹⁰ except that the function of the "writing element" was assumed here not by an optical image gliding over the photographic film, but a current sheath propelled over the coating by the Lorentz force. This method made it possible to register individual current elements with dimensions up to $20 \mu\text{m}$.

Following the initiation of the breakdown by the laser plasma, a glowing current sheath distributed over the expanding laser plasma was produced near the axis of the interelectrode gap. The first pinch effect was observed after 60–100 nsec [Fig. 2(a)]. The succeeding decay of the plasma column led to a repeated filling of the interelectrode gap with plasma and to the onset of

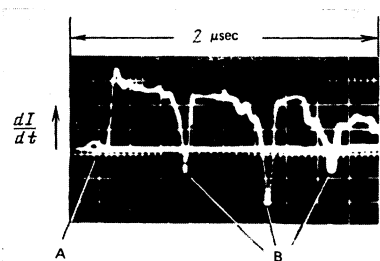


FIG. 2. Signal of the time derivative of the current.

a secondary current sheath, which was in turn accelerated towards the axis and collapsed. The first closing of the current sheath contracting towards the axis occurred near the end face of El_1 [Fig. 1(b)], after which the pinching process propagated along the axis. After penetrating through the central opening in El_2 , the current sheath "splashed out" from the interelectrode gap, forming a spouting current sheath [Fig. 1(c)]. The current flow was accompanied by heating of the electrodes. The voltage drop across the plasma at the instant of pinching ignited an arc and changed the process into an arc-discharge stage which is of no interest for the present research. If the conditions for igniting the arc were not satisfied, the decay and the subsequent contraction of the interelectrode plasma were repeated. The number of secondary "decay-contraction" cycles could change from discharge to discharge in a range 1–3 [Fig. 2(B)]. Each of the contractions was accompanied by flashes of microwave and x radiation and led to filling of the axial region with a dense plasma. To simplify the analysis, we discuss hereafter in the present paper results obtained in the case of discharges that have after the contraction (A) (whose effect was negligible in view of the smallness of the current at the instant of this pinching only one contraction (B).

The pinching produced in the entire axial region of the interelectrode gap a dense nonuniform plasma with values of n_e and T_e that varied randomly along the axis. A number of regions in the produced plasma had parameters greatly exceeding the values averaged over the pinching region. Such local high-temperature plasma formations could occur at arbitrary points near the axis. For the sake of convenience, we investigated in the course of the experiments mainly high-temperature plasma formations produced in two regions of the space near the electrodes, in the region near the end face of El_1 (which we shall call axial) and in the near-axis region around El_2 (the halo region). In the axial region, the high-temperature plasma formation was produced in 80% of the discharges [Fig. 1(b)], and 20% in the halo region [Fig. 1(c)]. A characteristic property of the local high-temperature plasma formations from the halo region is their "comet-like" shape. The "tails" of the recorded local high-temperature formations duplicated the bend in the spouting current sheath. When the observation region was gradually moved along the axis from the axial region into the halo region, the parameters of the local high-temperature plasma formations changed monotonically, thus confirming that they have a common "origin."

The picture of the traces left by the current sheath on the coatings deposited on the El_2 surface constituted a series of tracks. Starting from the inner surface of El_2 near the acute-angle ledge on El_1 , the tracks were directed along the axis and were registered up to the external end face of El_2 [Fig. 1(d)]. The transverse dimension of an individual track decreased from $\sim 300 \mu\text{m}$ at the initial stage to $\sim 150 \mu\text{m}$ in the final phase of motion of the current sheath. A considerable fraction of the tracks were grouped in pairs. We registered on the average ~ 10 pairs of tracks on the outer side of El_2 . The observed picture of the tracks was the result of the

existence of a fine structure in the current-carrying plasma—the breakup of the plasma into individual current filaments. A comparison of the tracks left by the spouting current sheath on the outer side of the end face of EI_2 with the images of the local high-temperature plasma formations recorded on film in a pinpoint camera in the halo region has shown that their transverse dimensions are close in value. It is obvious that the models based on the notion that the current-carrying pinching plasma is a locally uniform plasma column subject to a “neck” type instability cannot be used to explain the onset of the local high-temperature plasma formations in the halo region and their shapes observed in our case. A reliable approach is the one used in Ref. 11, where the model that explains the onset of the local high-temperature plasma formations starts from consideration of the process that evolves in the region of the initial linkup of the current filaments that make up the fine structure of the current-carrying plasma. (The prior linkup is stipulated because the processes that ensure the energy dissipation observed here should cause rapidly enough, within a time of the order of the time of formation of the hot core of the local high-temperature plasma formation, the current that flows through the linking current filaments to drop to a level below the critical value at which the energy-input process is still significant.)

The filamentary structure of the current-carrying plasma is observed in practically all types of strong-current pinching discharges: the z -pinch and θ -pinch,¹² the Mather plasma focus,¹³ the Filippov plasma focus geometry,¹⁴ and others. This phenomenon was most thoroughly investigated in Refs. 13 and 15–17. An important result of these investigations was the observation of the effect of self-stabilization of the fine structure on account of the development, in each of the current filaments, of intrinsic longitudinal magnetic self-fields¹⁵ B_z .

Since it is “frozen” in the current-filament plasma, B_z is a stabilizing factor that prevents the development of instability of the “neck” ($m=0$) and “snake” ($m=1$) type. The filaments are the main channels that ensured the passage of the interelectrode current. The lifetime of an individual filament can amount to several microseconds. Its transverse radius is close to the Larmor radius (ρ_z) of the ion revolving with thermal velocity in the field B_z . In this case $B_z < B_\theta$, where B_θ is the azimuthal magnetic field of the filament current. Correspondingly $\rho_z > \rho_\theta$, where ρ_θ is the Larmor radius of the ion in the field B_θ . Both possible directions of B_z inside the current filament are equally probable and do not depend on the polarity of the electrodes. The filaments are produced in pairs, and the direction of B_z is opposite in the paired vortices.

PARAMETERS OF LOCAL HIGH-TEMPERATURE PLASMA FORMATIONS

The electron temperature of a local high-temperature plasma formation in the axial and halo regions was measured by the filter method¹⁸ for the case of electrodes made of copper. The pickups for the x rays were sim-

ultaneously operating three “filter–scintillator–light pipe–photomultiplier–oscilloscope” channels. A plastic (β -terphenyl in polystyrene) scintillator an FÉU-87 photomultiplier, and an S8-12 oscilloscope were used. The temporal resolution of the pickups at the half-maximum level was 7 nsec. The dynamic range of the recording system was 5–6 orders of magnitude. It was achieved by varying the supply to the photomultiplier and by varying the distance from the pickup to the local high-temperature plasma formation. The appreciable length of the light pipes and careful screening of the photomultiplier made it possible to eliminate induced signals that occur in the recording circuits at the instant of pinching. The cutoff energies (E_{cut}) of the aluminum filters were chosen in the range $T_e \ll T_{\text{cut}} < E_b$, where the upper limit is the spectral-distribution inflection point that separates the sections in which thermal (recombination radiation of thermal electrons) and superthermal (bremsstrahlung of superthermal electrons present in the region of the local high-temperature plasma formations) radiation predominate. In the preliminary experimental run it was found that $E_b \approx 100$ keV. The chosen values of E_{cut} were 30, 60, and 80 keV. The calculations were based on relative measurements. The arithmetic mean of three possible values was taken to be the true one. The deviation of each of the values from the mean did not exceed 15% in this case. The values obtained in this manner were averaged over a segment of ~ 7 nsec (the time resolution of the recording apparatus). Figure 3 shows histograms of T_e for the local high-temperature plasma formations produced in the axial region. The histograms were plotted for three selections of 30 values each. Each selection pertains to a definite value of the discharge current at the instant of formation of the local high-temperature plasma formation (I) at a constant value $I_{\text{max}} = 200$ kA. At larger values of I we observed larger values of T_e . The appreciable spread of the registered values of T_e ($\Delta T_e / T_e \approx 1$) indicates that the processes causing the local high-temperature plasma formations are stochastic. The values of T_e for formations from the halo region were on the average smaller by a factor 3–5 than for the axial region. The instant of appearance of a signal from the x-ray pickup that “views” the halo region was delayed on the average ~ 30 nsec relative to the onset of the signal in the axial region. (This delay gives a pinching-region propagation velocity $\sim 3 \times 10^7$ cm/sec.)

To investigate the structure and dimensions of the local high-temperature plasma formation in the axial

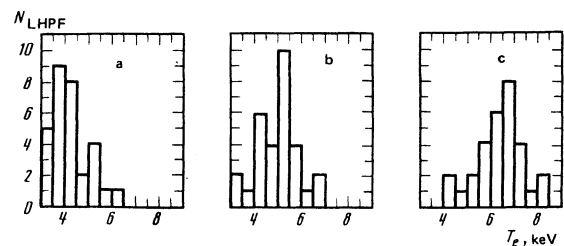


FIG. 3. Histogram of T_e of local high-temperature plasma formations from the axial region for different values of the discharge current at the pinching instant at $I_1 = 100$ (a), $I_2 = 120$ (b), and $I_3 = 140$ kA (c); $I_{\text{max}} = 200$ kA.

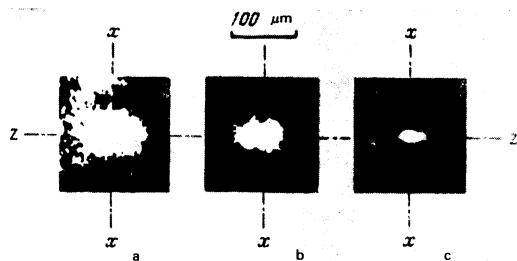


FIG. 4. Pictures of local high-temperature plasma formations obtained with x rays of various hardnesses at $E_{\text{cut}} = 2$ (a), 3 (b), and 4 keV (c).

region we used simultaneously three pinpoint cameras with 12- μm diameter holes. The x-ray image was photographed on UF-VRR film placed parallel to the discharge axis. The distance from the axis to the diaphragm and from the axis to the film were respectively 15 and 30 mm. The spectral range of the registered radiation was determined by the thickness of the beryllium filters placed in front of the stop openings. The pinpoint photographs of an individual local-temperature plasma formation, registered at different filter thicknesses, are shown in Fig. 4. With increasing hardness of the registered quanta, the average size of the formation photograph decreased monotonically, amounting to 40, 30, and 25 μm in the transverse direction. The longitudinal dimension was 1.5–2 times larger than the transverse. The transverse dimension of the hottest region turned out to be comparable with the resolution of the pinpoint camera, namely $\sim 25 \mu\text{m}$. This value will be used hereafter in the estimates as the averaged transverse dimension of the hot core of the local high-temperature plasma formation. Because of the low value of T_e in the formations produced in the halo region, they could be photographed with pinpoint camera only at filter cutoff energy 2 keV. In this case the characteristic linear dimensions of the images were 50–300 μm .

The pinpoint photographs obtained for the axial region make it possible to describe in this case individual local high-temperature plasma formations as aggregates of plasma ellipsoids of revolution imbedded in one another with an axis ratio 1.5–2 and with an electron temperature that increases towards the center. The monotonic character of the variation of the image of the formation with increasing hardness of the registered x-ray quanta indicates that such a plasmoid is locally uniform. Accordingly, it can be proposed that the local high-temperature plasma formations are produced as a result of some "elementary" interaction between the current and the plasma and the aggregate of these interactions ensures integral heating of the pinching region.

Since no temporal resolution is provided in the pinpoint-camera technique, the model of a local high-temperature plasma formation with plasma parameters that increase towards the center can serve as a picture of the instantaneous state of the formation, as well as describe the succession of states that appear in the course

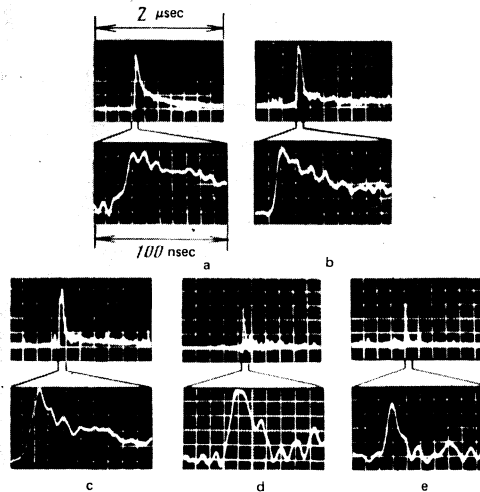


FIG. 5. Oscillograms of pulses of x rays of different hardness, produced by the onset of a local high-temperature plasma formation in the axial region at $E_{\text{cut}} = 3$ (a), 8 (b), 20 (c), 50 (d), and 100 keV (e).

of the expansion (contraction). Additional information is provided by the results of an investigation of the temporal evolution of the x radiation. The oscillograms of the axial-region signals obtained at the output of the x-ray pickups (Fig. 5) took the form of packets of weakly resolved pulses with a steep rise and gently sloping descent. The duration of the packet front makes it possible to estimate the upper limit of the existence of a hot region of the local high-temperature plasma formation at $t \lesssim 10 \text{ nsec}$. The speed of sound (c_s) in the plasma in the hot region, in which the plasma would decay in the case of free expansion, is $\sim 10^7 \text{ cm/sec}$ and leads to characteristic inertial containment times $t_{\text{in}} \approx 10^{-12} \text{ sec}$. This is much shorter than the observed electron-temperature relaxation times estimated from the durations of the decay of the x-ray pulses. It can be assumed that the process starts with an abrupt increase of T_e and the onset of a hot core, followed, in the presence of a "retarding" axial magnetic field, by a comparatively slow expansion of the local high-temperature plasma formation, accompanied by cooling.

To estimate the electron density in the region of the local high-temperature plasma formation, we use the Bennett relation,¹⁹ the validity of which for the investigated case was confirmed earlier²⁰ in a number of experiments:

$$I = (4\pi c^2 r^2 n_e \bar{T})^{1/2} \approx (4\pi c^2 r^2 n_e T_e)^{1/2},$$

where r , c , and \bar{T} are respectively the current-channel radius, the speed of light, and the average temperature.

Frame-by-frame photography has shown that in the axial region, where the geometry of the electrodes ensured primary joining-together of the collapsing current sheath, the diameter of the current channel decreases to a value close to the resolution of the recording apparatus ($\sim 0.7 \text{ mm}$). It can be assumed that the conditions are satisfied here for the simultaneous link-

up of the bulk of all the filaments that form the current sheath. Naturally, the greater part of the discharge current could flow through a channel with transverse dimensions close to the hot region of the local high-temperature plasma formation. In the halo region, the overall transverse dimensions of the spouting current sheath were not less than 3 mm. What was more probable here is the simultaneous joining of only a fraction of the channels—a current concentrated in two or more filaments could flow through the local high-temperature plasma formation. Using the previously obtained values for the parameters of the core of the formation from the axial region ($T_e \approx 6$ keV, $2r \approx 25$ μ m, $I \approx 140$ kA), we obtained $n_e \approx 2 \cdot 10^{21}$ cm $^{-3}$. For the halo region ($T_e \approx 2$ keV, $2r \approx 80$ μ m, 14 kA $\leq I \leq 140$ kA) we have $4 \cdot 10^{18}$ cm $^{-3} \leq n_e \leq 4 \cdot 10^{20}$ cm $^{-3}$.

MECHANISM OF ENERGY TRANSFER TO THE PLASMA

The presence of a fine structure of the current sheath leads to a situation in which $2\rho_\theta$, being much smaller than the overall dimensions of the current-carrying plasma, becomes comparable with the characteristic linear plasma dimension, which is determined by the radius of the current filament. The use of the equations of macroscopic magnetohydrodynamics in their usual form, particularly for the compression stage—the classical “snowplow” model—is no longer correct. We introduce a parameter that characterizes the degree of this “incorrectness”: $\alpha = r/\rho_\theta$. We consider the scheme of the collapse of a current sheath, taking into account the self-stabilization of its fine structure. We assume that the current sheath consists at the instant of pinching of two current filaments that carry internal longitudinal magnetic fields of equal magnitude and opposite direction, and moving towards the discharge axis from opposite sides with velocity $\pm V_k$ (Fig. 6, left). (In the experiment we registered in the compression stage approximately 10 pairs of current filaments. The presented reasoning can be easily applied to this case if it is assumed that the condition

$$\sum_i B_z^i \approx 0 \quad (1)$$

is satisfied, where i numbers the current filaments that participate in the linkup. The latter should be satisfied

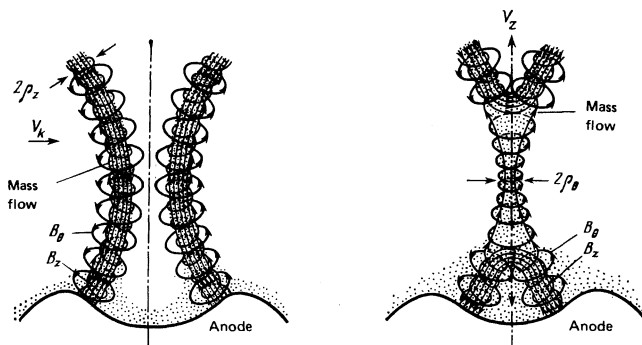


FIG. 6. Diagram showing the merging of vortical self-stabilized current filaments (with left-hand and right-hand rotation).

because both directions of B_z are on a par.²¹ The pressure balance on the surface of an individual current filament prior to the linkup will correspond to the expression

$$(N_i T_i + N_e T_e) + r^2 B_z^2 / 2 = I_f^2 / 2c^2, \quad (2)$$

where T_i, N_i, N_e, I_f are respectively the ion temperature, the ion and electron linear densities, and the filament current. The joining of the filaments (Fig. 6, right) leads to a reconnection of the force lines of B_z and to their “departure” with velocities $\pm V_k$ along the discharge axis. The last term in the left-hand side of (2) then vanishes, the existing pressure balance is upset, and contraction of the channel begins. According to the expression²²

$$I \sim e N_e c_s / \alpha,$$

where e is the electron charge, as α approaches unity the electron drift velocity approaches c_s . The excess of the drift velocity over c_s produces conditions for Čerenkov buildup of ion-sound turbulence. When ion-sound waves appear, the current electrons are slowed down by collisions with the plasma particles, and interaction with the plasma waves produces an anomalous resistance revealed by the abrupt minimum of $\Delta(dI/dt)$ on the signal representing the time derivative of the current (Fig. 2).

The value of $\Delta(dI/dt)L$, where L is the inductance of the discharge circuit, was ~ 10 kV in the experiment; this yields for the electric field intensity in the plasma of the local high-temperature plasma formation⁸ a value $\varepsilon \approx 10^6$ V/cm. This fits well in the range of ε :

$$2 \cdot 10^4 \text{ V/cm} = \frac{m_e N_D}{m_i \cdot 100} \varepsilon_a < \varepsilon < \frac{N_D}{100} \varepsilon_D = 3 \cdot 10^7 \text{ V/cm},$$

where N_D and ε_D are respectively the Debye number and the Dreicer field intensity at which intense ion-sound turbulence develops, with frequencies

$$10^9 \text{ sec}^{-1} \approx \frac{2ZeI}{m_i c^2 r} \approx \frac{ZeB_\theta}{m_i c} \approx \omega_{H_i} < \omega_i < \omega_{p_i} = \left(\frac{4\pi Z^2 e^2 n_i}{m_i} \right)^{1/2} \approx 10^{11} \text{ sec}^{-1}, \quad (3)$$

where ω_{H_i} , ω_{p_i} , and Z are respectively the gyrofrequency of the ions in the field B_θ , the ion plasma frequency, and the average ion charge.²³ The frequency of the ion-ion collisions, $\nu_i \approx 10^9$ sec $^{-1}$, is less than ω_s for the case of local high-temperature plasma formations, and the dissipation of the produced oscillations is ensured by Landau damping with limitation of the length of the “train” of the ion-sound waves to a value ~ 70 wavelengths²⁴ (the second ion-sound wave damping mechanism, collisions, is significant at $\omega_s < \nu_i$). The fact that in this case the electron component is primarily heated, and accordingly a difference between the electron and ion temperatures is maintained, leads to a regular restoration of the buildup of the dissipating wave. The pulsations that are produced in this manner ensure in the upshot a self-sustaining quasistationary turbulent state. Relaxation of such a state is possible when the current is decreased in the course of the expansion of the turbulence region, which has an anomalously high resistance.

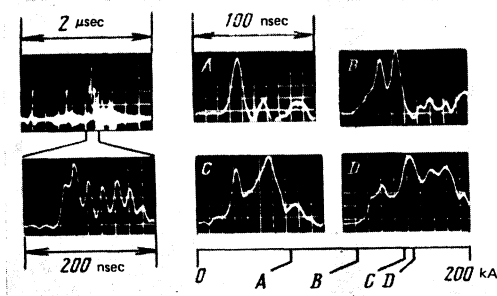


FIG. 7. Oscillograms of pulses of microwave radiation at frequency 10 GHz, produced at the instant of the onset of local high-temperature plasma formation in the axial region (at various values of I).

MICROWAVE RADIATION FROM THE REGION OF THE LOCAL HIGH-TEMPERATURE PLASMA FORMATION

The excited ion-sound waves can be transformed in the case of nonlinear interactions into electromagnetic waves. This conversion is possible without a substantial change in the frequencies—the frequencies of the radiation for the plasma turn out to be close to the measured frequencies of the excited plasma oscillations.²⁵ To register the radiation from the interelectrode region at frequencies in the range (3) we used in the experiment a detector head with a crystal diode. The pickup registered a section of the microwave spectrum near the frequency $\omega \approx 10^{10} \text{ sec}^{-1}$ with a time resolution 7 nsec. The radiation intensity (J_ω) recalculated for the total solid angle amounted at the onset of the local high-temperature plasma formation to $\approx 100 \text{ W}$. The radiation signal took the form of a packet of pulses (Fig. 7) with total duration 10–100 nsec and with intervals $\sim 15 \text{ nsec}$ between individual spikes. The amplitude and duration of the packet correlated with the simultaneously registered quantities I and $\Delta(dI/dt)$. The measured value of J_ω exceeds by more than six orders of magnitude the corresponding value obtained from Planck's formula (J_ω^p) assuming plasma equilibrium in the region of the local high-temperature plasma formation. Accordingly

$$\frac{T_{\text{eff}}^{\omega}}{\pi\lambda^2} = J_\omega \gg J_\omega^p = \frac{T}{\pi\lambda^2}, \quad T_{\text{eff}}^{\omega} \gg T, \quad (4)$$

where λ , T , and T_{eff}^{ω} are respectively the radiation wavelength, the equilibrium-plasma temperature, and the effective temperature of the radio emission. The inequality (4) is the condition for the existence of developed turbulence at the plasma-wave modes with frequency ω (if the aforementioned condition for the conversion of plasma waves into electromagnetic radiation is satisfied). The fact that the duration of the microwave-radiation packet is large compared with the time of the onset of the hot core of the local high-temperature plasma formation offers evidence that in the course of the collapse the processes take place not in one but in a number of localized sections of the region where the current sheath is joined together. The registered duration $\Delta t \approx 10 \text{ nsec} \approx 70 \omega^{-1}$ of the individual spikes can be attributed to Landau damping of the produced plasma waves.

ACCELERATION OF PARTICLE FROM THE LOCAL HIGH-TEMPERATURE PLASMA FORMATION REGION

A general property of a turbulent plasma, besides the anomalously high level of microwave radiation, is the generation of fast particles. Ion-sound waves turn out to be particularly effective for the acceleration of heavy multiply charged ions,²⁶ intense fluxes of which from the local high-temperature plasma-formation region were observed in Ref. 27. To register the ion component of the plasma expanding from the interelectrode region we used in the experiment a charge collector and a time-of-flight spectrometer in combination with magnetic mass analyzer, with mass and charge resolution ~ 100 . The ion spreading in both the longitudinal and transverse directions was investigated. After pinching, the plasma-column decay products passed through the central opening in El_2 or through a lateral opening in the coaxial part of El_2 along the time-of-flight analyzer and landed on the charge collector or on the input slit of the magnetic mass spectrometer. The detector used at the exit from the latter was an open-type VEU-1A secondary electron multiplier. The sensitivity threshold of the entire system, determined by the "angle of view" of the secondary electron multiplier and by the energy resolution of the magnetic mass spectrometer was, assuming isotropic expansion, $\sim 10^9$ particles per pulse. We investigated electrode pairs made of the metals Al, Fe, Cu, Mo, W, and Pb. The oscillograms of the mass spectra constituted a series of peaks, each of which corresponded to a definite Z/m_i ratio. The time position of the peak, at the known time-of-flight, made it possible to determine the peak position on the energy scale. To plot the total energy spectrum, the measurement was made at 20 different values of the magnetic field of the spectrometer.

The ion component registered in the axial observation direction had a clearly pronounced fast component with particle energies $E_i > 10 \text{ keV}$, and a slower component with $E_i < \text{keV}$. The origin of the slow ion component was determined by observing the variation of the collector signal due to the decay products of the interelectrode plasma with I_{max} increased gradually from discharge to discharge. The charge collector was mounted in the axial direction at a distance 75 cm from the local high-temperature plasma formation. At zero current, the collector registered by ion component of the expanding laser plasma. Passage of the discharge current led to the appearance of the fast component and to a distortion of the slow-component signal. The resultant current sheath constituted two current-carrying surfaces that moved apart along the axis in opposite directions. The turbulization regions produced at the points of intersection of the discharge axis with the surfaces heated in the course of motion and dragged behind them part of the laser plasma remaining in the corresponding half-spaces of the interelectrode gap. As a result, part of the collector signal was cut off—it was carried away towards the internal electrode, and in the cutoff region a spike was produced, corresponding to the additional ionization due to the expanding turbulence region. With increasing I_{max} , the rates of linkage of the current sheath decreased, leading to a displacement of the turbulent

region to the front of the laser plasma. At $I_{\max} \approx 200$ kA the amplitude of the perturbation produced by the turbulent piston was larger by two orders of magnitude than the initial signal amplitude observed from the laser plasma. This points to the presence of an energy difference, larger by more than two orders of magnitude, transferred to the plasma on account of the secondary turbulent and primary laser heating mechanisms. The presented picture of the interaction of the expanding plasma with the turbulization region was the result of the first contraction [Fig. 2(A)]. A similar process took place also in the course of the succeeding contractions, the only difference being that the role of the laser plasma was assumed here by the secondary plasma eroded in the interelectrode gap from the surfaces of the electrodes by the flowing current.

A characteristic feature of the fast component was its high degree of ionization. The fast particles contained ions with all charges, from single to Al^{+11} , Fe^{+18} , Cu^{+19} , Mo^{+20} , W^{+25} , and Pb^{+26} . The ionization energies of the latter reached 800 eV, and they were correspondingly produced and accelerated in the low-temperature regions of the plasma produced upon pinching. These regions were the local high-temperature plasma formations produced in the course of the secondary contractions [Fig. 2(B)]. (The mass-analyzer registration threshold did not make it possible to observe ions with the largest ionization multiplicity, which can be registered here by spectroscopic methods.⁶⁾ The energy spectrum of the singly charged ions of the fast component had a maximum at energies of several dozen keV and extended to energies ~ 1 MeV. Ions with larger charges had a higher average energy at a lower width of the observed-energy spectrum. With increasing ionization multiplicity, the number of registered ions decreased. For the maximum charge numbers, it was smaller by 5–6 orders than for the singly charged particles. When the observation was in the transverse direction, the registered number of fast ions was smaller by several orders than in longitudinal observation. In this case much lower average ion energies were registered at a lower ionization multiplicity.

It is known²⁴ that the largest effective buildup of ion-sound waves, which are longitudinal, takes place along the applied external field (in the investigated case, along the system axis). The ions accelerated in this case have velocities directed along the wave vector of the wave, and energies larger than T_e . The maximum rate of acceleration occurs at an energy several times T_e and decays like $E_i^{-3/2}$. The registered anisotropy of the acceleration process, as well as the characteristic shape of the energy spectra correspond qualitatively to the mechanism of acceleration by ion sound. A confirmation of the turbulent character of the acceleration process is in this case the large width of the energy spectrum—the ions accelerated stochastically by random fields of turbulent pulsations should have a broad energy spectrum. Another proof of the decisive role of the collective acceleration mechanisms is the independence of the observed picture on the polarity of the electron. In an earlier study²⁸ of a Mather plasma focus with discharge-circuit parameters close to those in the present

experiment, using a Thomson spectrometer, they registered directly the periodic structure of the energy spectrum of fast ions which is typical of the case of acceleration of plasma waves.

CONCLUSION

The investigations of the plasma produced in the region of linkage of the current sheath of a strong-current vacuum discharge have shown that it was possible to separate in its volume individual plasmoids with parameters n_e and T_e considerably exceeding the average values over the pinching region. Such local high-temperature plasma formations had, within the limits of the resolution of the recording apparatus, local homogeneity, i.e., they resulted from a separate action on the plasma by a mechanism that ensures transfer of the current energy to the plasma.

The measurements and estimates of the local high-temperature plasma-formation parameters have shown this process to be highly effective. The proposed model of the local action on the plasma as the starting instant of effective dissipation of the current energy considers the start of the disruption of the self-stabilized fine structure of the current-carrying plasma. The pinching process is described as the transition of the plasma from a state in which its characteristic linear dimension $2r$ (diameter of the current filament) is close to $2\rho_e$, into a state with $2r \approx 2\rho_0$. The place where this transition takes place is the region of the linkup of the filaments that satisfy the condition $\sum_i B_z^i \approx 0$. The fact that the electron drift velocity reaches the ion-sound velocity ensures Čerenkov buildup of plasma turbulence accompanied by an anomalously high heating of the plasma. The results of the investigation of the microwave radiation and of the ion fluxes from the interelectrode region confirm qualitatively the proposed model. Another confirmation of the correctness of the model was the fact that optimization of the electrode geometry (with an aim at localizing the region of initial linkup of the filamentary current structure) had resulted in spatial stabilization of the onset of the local high-temperature plasma formations. A filamentary structure of a current-carrying plasma is observed in particularly all types of strong-current pinched discharges. Accordingly, the results of the present investigation can be of interest also for larger installations operating in the mega-ampere range of discharge currents.²⁹

In conclusion, the authors thank G.A. Sheroziya, and Yu. Ya. Lapitskiĭ for collaborating in the organization of the experiment, as well as D.A. Uzienko and A.N. Oblizin for help with the investigation.

¹⁾The current filaments that make up the current-carrying plasma in strong-current pinched discharges are gasdynamic vortices whose rotation leads to the onset of internal self-fields B_z (only the ion component participates in the rotational motion—the light electrons are “tied” to the force lines of B_z).

²⁾The condition (1) at the instant of pinching may be satisfied in not all discharges, since the process of formation of the current sheath is stochastic. In this case partial annihilation of the fields B_z will take place in the course of the con-

traction, while the residual field can be registered. It appears that the effects reported in Ref. 21, where the presence of a field B_z was observed in 20% of the discharges in the pinching state, is one of these cases.

- ¹L. Cohen, U. Feldman, M. Swartz, and J. H. Underwood, *Opt. Soc. Amer.* **58**, 843 (1968).
- ²J. W. Mather, *Phys. Fluids* **8**, 366 (1965).
- ³J. Shiloh, A. Fisher, and N. Rostoker, *Phys. Rev. Lett.* **40**, 515 (1978).
- ⁴J. Fukai and E. J. Clothiaux, *Phys. Rev. Lett.* **34**, 863 (1975).
- ⁵W. A. Cilliers and R. U. Datla, *Phys. Rev. A* **12**, 1408 (1975).
- ⁶C. R. Negus and N. J. Peacock, *J. Phys. D* **12**, 91 (1979).
- ⁷E. D. Korop, B. É. Meĭerovich, Yu. D. Sidel'nikov, and S. T. Sukhorukov, *Usp. Fiz. Nauk* **129**, 87 (1979) [*Sov. Phys. Usp.* **22**, 727 (1979)].
- ⁸A. Cernard, A. Coudeville, J. P. Garconnet, A. Jolas, J. Mascureau, and G. Nazet, *Plasma Phys. and Cont. Nucl. Fusion Res. (Proc. 6-th Int. Conf., Berchtesgarden, 1976)* **3**, IAEA, Vienna (1977), p. 491.
- ⁹G. Herziger, L. Bakowsky, W. Peschko, and F. W. Linder, *Phys. Lett.* **4**, 273 (1978).
- ¹⁰E. K. Zavoĭskiĭ and S. D. Fanchenko, *Dokl. Akad. Nauk. SSSR* **108**, 218 (1956) [*Sov. Phys. Dokl.* **1**, 265 (1957)].
- ¹¹U. S. Bykovsky and V. B. Lagoda, *Proc. 10-th Eur. Conf. Cont. Plasma Phys.*, Moscow, **1**, D9 (1981).
- ¹²I. F. Kvartskava *et al.*, 1-st IAEA Conf. Plasma Phys. and Cont. Nucl. Fusion Res., Salzburg, 1961, p. 533.
- ¹³W. H. Bostick, V. Nardi, and W. Prior, *Proc. Conf. Cosmic Plasma Phys.*, ESEIN, Frascati, 1971 (N. Y. Plenum Press), p. 175.
- ¹⁴V. A. Gribkov, O. N. Krokhin, G. V. Sklizkov, V. V. Filippov, and T. I. Filippova, *Pis'ma Zh. Eksp. Fiz.* **18**, 11 (1973) [*JETP Lett.* **18**, 5 (1973)].
- ¹⁵W. H. Bostick, V. Nardi, and W. Prior, *Annals NY Academy Sciences* **251**, 2 (1975).
- ¹⁶V. Nardi, *Phys. Rev. Lett.* **25**, 718 (1970).
- ¹⁷W. H. Bostick, V. Nardi, and W. J. Prior, *Plasma Phys.* **8**, 7 (1972).
- ¹⁸T. P. Donaldson, *Plasma Phys.* **20**, 1279 (1978).
- ¹⁹W. H. Bennet, *Phys. Rev.* **45**, 89 (1934).
- ²⁰T. N. Lie and R. C. Elton, *Phys. Rev. A* **3**, 865 (1971).
- ²¹E. M. Gordeev, P. V. Kuksov, L. I. Rudakov, and S. D. Fanchenko, *Pis'ma Zh. Tekh. Fiz.* **6**, 1450 (1980) [*Sov. Tech. Phys. Lett.* **6**, 625 (1980)].
- ²²Yu. A. Bykovskiĭ, V. B. Lagoda, and G. A. Sheroziya, *Pis'ma Zh. Eksp. Teor. Fiz.* **31**, 265 (1980) [*JETP Lett.* **31**, 243 (1980)].
- ²³S. M. Hamberger *et al.*, 9th Int. Conf. Phen. Ion Gases, 1969 (Cont. Papers, Bucharest, 1969), p. 570.
- ²⁴S. A. Kaplan and V. N. Tsytovich, *Plazmennaya astrofizika (Plasma Astrophysics)*, Moscow, Nauka, 1972.
- ²⁵E. A. Kornilov, O. F. Kovnik, Ya. B. Faĭnberg, L. I. Bolotin, and I. F. Kharchenko, *Vzaimodeĭstvie puchkov zaryazhennykh chastits s plazmoĭ (Interaction of Charged-Particle Beams with Plasma)*, No. 7, Kiev, Naukova Dumka, 1965, p. 36.
- ²⁶E. K. Zavoĭskiĭ and L. I. Rudakov, *Fizika Plazmy (Kollektivnye protsessy i turbulentnyĭ nagrev) [Plasma Physics (Collective Processes and Turbulent Heating)]*, Moscow, Nauka, 1967.
- ²⁷Yu. A. Bykovskiĭ, V. B. Lagoda, and G. A. Sheroziya, *Pis'ma Zh. Eksp. Teor. Fiz.* **30**, 489 (1979) [*JETP Lett.* **30**, 458 (1979)].
- ²⁸H. Krompholz, E. Grimm, F. Rühl, H. Schönbach, and G. Herziger, *Phys. Lett.* **76A**, 255 (1980).
- ²⁹Yu. A. Bykovskiĭ, V. B. Lagoda, and A. N. Oblizin, *Pis'ma Zh. Eksp. Teor. Fiz.* **35**, 139 (1982) [*JETP Lett.* **35**, 168 (1982)].

Translated by J. G. Adashko